Fibrin Microbeads (FMB) as Biodegradable Carriers for Culturing Cells and for Accelerating Wound Healing[1]

Raphael Gorodetsky, Richard A. F. Clark,* Jianqiang An, James Gailit,* Lila Levdansky, Akiva Vexler, Elisha Berman, and Gerard Marx†

Sharett Institute of Oncology, Hadassah University Hospital, Jerusalem, Israel; *Department of Dermatology, SUNY Medical School, Stony Brook, New York, New York, U.S.A.; †Vitex Inc, New York, New York, U.S.A.

We have developed biodegradable fibrin-derived microbeads as potent cell carriers. The fibrin-derived microbeads, 50–200 μm in diameter, were tested for their attachment to a wide range of cell types. Fibrin-derived microbeads were shown to be greatly haptotactic to cells (such as endothelial cells, smooth muscle cells and fibroblasts), which respond to fibrinogen in contrast to keratinocytes and different cell lines derived from leukocytic lineage. The cells on fibrin-derived microbeads could be maintained for more than 10 d and achieved a high density. ^{31}P-nuclear magnetic resonance was employed to monitor phosphate metabolism in cells, with densities on the order of 100 million cells per g of fibrin-derived microbeads. The ^{31}P-nuclear magnetic resonance adenosine triphosphate and phosphocreatine signals, equivalent to the signal obtained with perfused normal skin, indicated that metabolism of cells on fibrin-derived microbeads was responsive to oxygenation and nutrients. Light, fluorescent, and confocal laser microscopy revealed that the porous fibrin-derived microbeads accommodate up to 200–300 cells due to their high surface area which minimized contact inhibition. Cells could degrade the fibrin-derived microbeads and be transferred to seed culture flasks without trypsinization. In a pig skin wound healing model, fibrin-derived microbeads + fibroblasts were transplanted into full thickness punch wounds. This procedure was compared with other treatment modalities, such as the addition of human platelet-derived growth factor BB or fibrin-derived microbeads alone. By the third day after wounding, only the wounds in which fibroblasts on fibrin-derived microbeads were added showed significant formation of granulation tissue. Based on the above, we project many uses of our novel fibrin-derived microbead technology for cell culturing, wound healing and tissue engineering. ***Key words: ^{31}P-nuclear magnetic resonance/fibrin(ogen)/haptotaxis/microcarriers/proliferation. J Invest Dermatol 112:866–872, 1999***

Fibrinogen and thrombin each exert proliferative and adhesive effects on cultured fibroblasts and other cells. Specifically, fibrin(ogen) and its various lytic fragments (i.e., FPA, FPB, fragments D and E) were shown to be chemotactic to macrophages, human fibroblasts, and endothelial cells (Lorenzet *et al*, 1992; Brown *et al*, 1993; Gray *et al*, 1993). Thrombin also has been shown to exert proliferative and adhesive effects on cultured cells (Shuman, 1986; Daniel *et al*, 1986; Bar-Shavit *et al*, 1990; Dawes *et al*, 1993). We showed previously that coating inert Sepharose beads (SB) with either fibrinogen or thrombin rendered them adhesive to a wide range of cell types. We used protein-coated SB to detect and grade the affinity of cells for the tested proteins and to screen normal and transformed cells for their haptotactic responses to fibrin(ogen) and thrombin (Gorodetsky *et al*, 1998).

Microcarriers beads made of some plastic polymers or glass provide cells with a surface area on the order of 10^4 cm^2 per liter for cell attachment, which is one order of magnitude larger than the area available with stack plates or multitray cell culture facilities (Griffith and Looby, 1997). From the point of view of transplantation biology, the major disadvantage of such cell microcarriers is that most of them are not biodegradable or immunogenic. Others have prepared microparticles from plasma proteins, such as albumin or fibrinogen, generally using glutaraldehyde to cross-link the proteins. Glutaraldehyde, however, is not appropriate for preparing cell culture matrices as such cross-linking slows down degradation of the matrix or blocks the protein epitopes, which may attract cells. Consequently, glutaraldehyde cross-linked microcarriers have been used mainly for drug release or imaging (Evans, 1972; Lee *et al*, 1981; Royer, 1982; Yapel, 1985; Miyazaki *et al*, 1986a, b, c; Arshady, 1990; Gref *et al*, 1994).

Based on our experience with the attraction of many normal cell types to fibrin(ogen) with minimal effect on their proliferation (Gorodetsky *et al*, 1998), we fabricated small particles (microbeads) of fibrin (FMB) to be used for high cell density culture. The fibrin(ogen), which is the main component of these beads, is not immunogenic and can be biodegraded within a few days. This paper describes the fabrication of FMB, the attachment and growth

Manuscript received October 12, 1998; revised December 28, 1998; accepted for publication February 24, 1999.

Reprint requests to: Dr. Raphael Gorodetsky, Sharett Institute of Oncology, Hadassah University Hospital, POB 12000, Jerusalem, 91120, Israel.

Abbreviations: HF, normal human fibroblast; fibrin(ogen), fibrin or fibrinogen; FMB, fibrin microbeads; SEM, scanning electron microscopy; SB, Sepharose beads.

[1]The authors declared conflict of interest. A patent on the method of preparation and commercial uses of FMB is pending.

Table I. Biochemical composition of fibrinogen source

	Pooled cryo	Pure fibrinogen[a]
Protein (mg per ml)	72 ± 10	41 ± 5
Fibrinogen (mg per ml)	13 ± 5	40 ± 5
Fibronectin (mg per ml)	3 ± 1	1 ± 1
IgG (mg per ml)	13 ± 2	trace
XIII (U per ml)	5 ± 1	20 ± 10

[a]Purified by fractionation.

of cultured cells on FMB, and their transplantation into an animal skin wound to accelerate healing.

MATERIALS AND METHODS

Fibrinogen Fibrinogen, prepared by fractionation of pooled plasma, has been virus inactivated by the solvent detergent (S/D) process and is a component of clinical grade fibrin sealant (Marx *et al*, 1996; Sanders *et al*, 1996). Cryoprecipitate was obtained from frozen and thawed pooled S/D plasma. The biochemical components of the fibrinogen sources are presented in **Table I**.

Thrombin Human thrombin (stock 200 U per ml) was prepared as described (Zou *et al*, 1997); its activity was determined by clot time assays calibrated against an international standard.

FMB preparation A typical preparation of FMB was carried out by heating 400 ml corn oil + isooctane (1:1) to 75°C with mechanical stirring. A solution of fibrinogen (25 ml; 40 mg per ml) or cryoprecipitate, diluted 1:4 in Tris/saline buffer (pH 7.4) with 5 mM Ca^{+2}, was mixed with thrombin to 5 U per ml (final concentration). The protein mixture was added to the heated oil at a rate so that the protein solution had not yet coagulated, and where the stirring dispersed the aqueous phase into oil-suspended droplets. Mixing and heating continued at ≈75°C for 6–8 h. The crude FMB was filtered off, washed with hexane, 95% ethanol, and air dried.

Solubility tests and sodium dodecyl sulfate–polyacrylamide gel electrophoresis (SDS–PAGE) The FMB were tested for solubility in Tris/saline or in 4 M urea. Neither the Tris buffer nor the 4 M urea dissolved FMB for up to 1 wk at room temperature. As FMB are not soluble, they were partially digested to obtain material for analysis. One hundred micrograms FMB were suspended in 1 ml 0.1 M NaOH, the supernatant samples were removed after 1 or 2 d and subjected to reduced 4–12% gradient SDS–PAGE (Nova, Encino, CA), using fibrinogen or normally clotted fibrin as controls.

Cell cultures The following cell types were used in this study: cultured normal human skin fibroblasts (HF) were isolated from skin biopsies of young human subjects and normal murine fibroblasts from the skin of 2–3 d old neonate C3H mice, as previously described (Gorodetsky *et al*, 1998), both cell types were grown for at least 12 passages. Syngeneic porcine fibroblast for wound healing experiments were grown up to three passages and isolated as previously described (Clark *et al*, 1996). Porcine smooth muscle cells were separated from thoracic aortas of young animals were grown up to 10 passages; normal human keratinocytes and normal bovine aortic endothelial cells from young animals were isolated and grown as previously described (Gorodetsky *et al*, 1998). Other cell lines tested were murine fibroblast line (3T3), murine leukemic cell line (p-388), human ovarian carcinoma line (OV-1063), murine mammary adenocarcinoma cells (EMT-6), and murine macrophage-like cell line (J774.2) all grown and maintained as previously described (Gorodetsky *et al*, 1998).

Culture medium components were purchased from Biological Industries (Beit-HaEmek, Israel) and fetal calf serum was supplied by GIBCO (Grand Island, New York, NY). The cell cultures were maintained at 37°C in a water-jacketed CO_2 incubator, and harvested by trypsin/versen solution with one to two passages per week in a split ratio of 1:10 for fast proliferating transformed cells and 1:4 for normal cell types.

FMB attachment assay The attachment of FMB to cells was compared with the cell response to fibrinogen-coated SB as recently described (Gorodetsky *et al*, 1998). Essentially, FMB were added to a growing culture and counted periodically by visual inspection with inverted phase microscope. Initially, all the beads freely rolled over the near confluent culture. At different time intervals, the fraction of beads anchored to the cells were counted (typically 300 beads but not less than 200 beads/plate) and the ratio of beads bound to the cells, relative to the total number of beads, was calculated. Experiments were carried out in triplicate.

Loading cells on FMB Prior to use, FMB were suspended in sterile alcohol for 1 h, rinsed in sterile saline, incubated in 0.1% azide overnight at 37°C and rinsed extensively with sterile saline. The cells to be loaded on the FMB were grown in large plastic tissue culture dishes in their normal growth conditions. Prior to reaching confluence, the cells were trypsinized, collected, and added to a number of 50 ml polycarbonate tubes, each with up to 1–10 million cells per 300 mg of beads suspended in about 6 ml of medium. The tubes were covered by perforated aluminum foil and loaded on a stand that slowly rotated the tubes at about 10 cycles per minute at an angle of 30°, so that the medium did not reach the perforated stoppers. The stand was placed in the CO_2 tissue culture incubator. A day after mixing the cells with FMB, the unattached cells were separated by brief vortexing, the tubes were kept still for 60–90 s to allow the FMB loaded with cells to sediment. The supernatant medium containing unattached cells as well as small fragments of FMB was removed and fresh medium added. The cells could continue growing on the FMB in the rotating device for more than 4 d.

For growth rate experiments with pig kidney epithelial cells, the serum content was set at 1%, 2%, 5%, and 10%. At regular intervals, a 100 μl sample was vortexed 3 s to disperse clumps, the particulate FMB allowed to settle (1 min) and the cell number was determined.

Assay for cell number Cell density was evaluated by the CellTitre 96Aqeous colorimetric assay (MTS assay) as previously described (Gorodetsky *et al*, 1998). Typically, the samples of 200 μl of suspended FMB + cells were placed in 24 well flat bottom plates (in triplicate) and 200 μl of freshly prepared mixture of MTS/PMS (CellTitre 96 AQueous Assay by Promega, Madison, WI) were added to each well; the plate was placed on a mechanical plate incubator shaker. After 2–6 h of incubation at 37°C, 0.1 ml of the supernatant was transferred to a 96 well plate. The optical density of the dye was read in a computerized automatic microwell plate spectrophotometer (Anthos HT-II, Salzburg, Austria) at 490 nm. The time points in which the optical density readings were within the optimal range, were chosen for the assay of cell density. For all cell types tested, the optical density readings of the MTS correlated well ($r > 0.97$–0.99) with the number of seeded cells.

Light, fluorescent and confocal laser microscopy Light and fluorescent microscopy was carried out using an Olympus Fluorescent Microscopy system at magnification range ×200–×860. Micrographs were taken by single or double (fluorescence and light) exposures.

A computerized confocal laser microscope (Zeiss Confocal Axiomate LSM410), using ×63 objective with double excitation at 410 and 543 nm, was used to visualize the endogenous fluorescence of the FMB and the cell nuclei stained with propidium iodide (PI). The FMB loaded with cells were fixed in 0.5% buffered glutaraldehyde. Before examination, 50 μg per ml PI was added in darkness for at least 20 min; the FMB were then placed on a microscope slide with phosphate-buffered saline/glycerol 80% and 2% DABCO, then scanned by the confocal microscope. The visual images (phase and differential interference contrast according to Nomarski) and the fluorescent slice scans were processed for overlap slice summation or 3D presentation.

Electron microscopy Samples of cells on FMB were fixed for scanning electron microscopy (SEM) by 2.5% glutaraldehyde, prepared by critical point drying, coated with osmium tetroxide, sputter coated with Au/Pd and examined with a Hitachi S-530 Scanning Microscope.

^{31}P-nuclear magnetic resonance (NMR) of cells loaded on FMB Fibroblasts, endothelial and EMT-6 cells were loaded on FMB (at about 100 million cells per g packed beads). About 1 g of FMB with cells were placed in a sterile NMR tube and perfused with the culture medium and a gas mixture of 95% O_2/5% CO_2 for up to 24 h. As a control, fresh mouse skin was cut into 2 mm wide strips, placed in the NMR tube and perfused with the medium. The 162 MHz ^{31}P-NMR spectra of the perfused samples were recorded on-line using Bruker AMX-400WB spectrometer (Sharoni *et al*, 1996). Spectra were acquired using scans accumulated with 1 s delay between the 45° pulses, spectral width of 8.5 kHz and 8000 data points. The intensity changes of the NMR resonances corresponding to inorganic phosphate (P_i), phosphocreatine (P_{Cr}) and the β-resonance of adenosine triphosphate (ATP) were recorded.

Pig skin wound healing model Full thickness excisional wounds were made by an 8 mm circular punch into the paravertebral skin of Yorkshire

pigs as previously described (Welch *et al*, 1990; Clark *et al*, 1996; McClain *et al*, 1996). To each wound space, 150 μl of 3 mg per ml fibrinogen mixed with 2 U per ml human α-thrombin were added. In some wounds, prior to the addition of the fibrin, 0.6–1.0 million of cultured human fibroblasts in suspension or on FMB were added to the bottom of the wound. As the wounds were harvested at day 3 after the addition of fibroblasts, rejection of xeno-implanted cells was not observed. In some wounds, human platelet-derived growth factor BB (PDGF-BB), a known chemotactic agent (Koyama *et al*, 1994) kindly provided by Ortho-McNeil (Princeton, NJ), was added to the fibrinogen/thrombin solution prior to applying it to the wound. Still other wounds received all additives. Wound sites were dressed with Tegaderm, a polyurethane occlusive dressing, and harvested after 3 d. Each formulation was tested in triplicate (n = 3).

Specimens from all wound sites were dissected vertically. One half was fixed with formalin, paraffin embedded, sectioned at 5 μm and stained with Masson trichrome to delineate morphologic alterations. The sections, which approximated the plane that vertically transected the center of each wound, were numerically coded and visually evaluated on a Nikon BHK-2 microscope by an observer who had not participated in the animal experiments.

Statistics The results of cell attachment and proliferation are represented as an average of two to four experiments. Mean values and standard errors were calculated for each point from the pooled normalized data. Statistical analysis of the significance of paired data was performed using the Student's t-test, assuming equal and unequal variance as dictated by the ANOVA test.

RESULTS

FMB characterization FMB fabrication generated about 60% weight/weight yield of FMB from starting protein solutions. The FMB were not soluble in either physiologic buffers or 4 M urea for up to 1 wk at room temperature. This suggests significant cross-linking of the proteins. In order to evaluate this directly, 100 μg FMB were digested in 1 ml 0.1 M NaOH for 1 or 2 d and the supernatant was analyzed by reduced SDS–PAGE and compared with control fibrinogen and fibrin. Densitometry of the gels showed that FMB contained many more cross-links than observed with normally clotted fibrin, which usually show only γ–γ dimers, loss of α and γ bands as well as α-α multimers (**Fig 1**).

Attachment of FMB to cells We monitored the propensity of FMB as well as Sb-Fib to be attached to the cells. Thus, either FMB or Sb-Fib were applied on to a near confluent human fibroblast culture and the proportion of beads that became attached to the cells were counted daily by phase contrast microscopy, as previously described (Gorodetsky *et al*, 1998). Control protein noncoated SB did not interact with the cells and floated freely in the culture medium even after prolonged incubation for up to a week (0% attachment). By contrast, by day 3, we observed that the attachment kinetics of FMB to fibroblasts were similar to the response elicited by SB-Fib (**Table II**).

The attachment of FMB to other normal and transformed cells corresponded to the cell interactions with SB-Fib (**Fig 2**, **Table II**). Cells such as keratinocytes, OV-1063, and J-774.2 did not significantly attach any of the beads; whereas transformed or normal human and murine fibroblasts as well as smooth muscle, endothelial, and EMT-6 cells attached the FMB with equal or greater degree than SB-Fib.

Rate of attachment of cells to FMB The kinetics of haptotactic response of fibroblasts, endothelial and smooth muscle cells to FMB (**Fig 2*A***) was similar to their responses to Sb-Fib (Gorodetsky *et al*, 1998). By day 3, most FMB were anchored to the cell layers.

Growth kinetics on FMB In the interest of observing the rate of cell proliferation on FMB, we monitored the growth of pig kidney epithelial cells on FMB maintained in culture medium containing from 1% to 10% serum (**Fig 2*B***) with twice weekly medium replacement. The results indicate that with 10% serum, a 7-fold increase in cell number could be achieved after 1 wk. By day 15, at the optimal conditions the cells had proliferated more that 30×. Cell proliferation at lower serum concentrations as recorded from day 10 onward was significantly lower ($p < 0.01$).

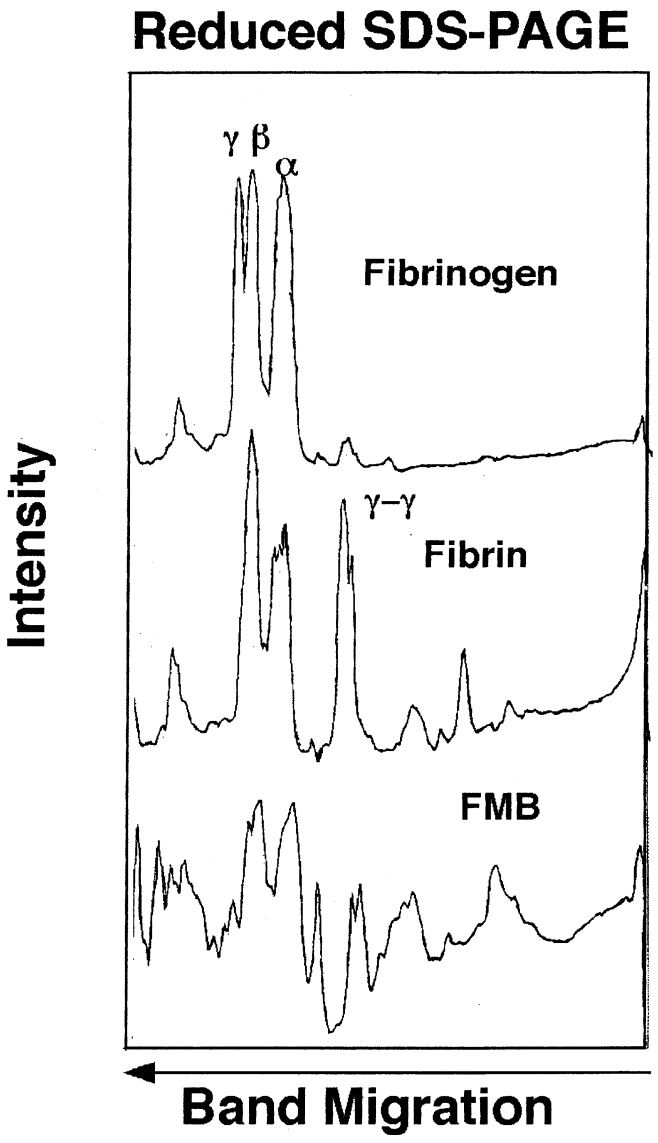

Figure 1. Densitometric tracings of reduced SDS–PAGE of: fibrinogen; fibrin; and partial NaOH digest of fibrin microbeads. It is apparent that the degree of fibrin cross-linking in FMB is much more extensive than in the fibrin clot as evident by the presence of high and low molecular weight fragments.

Table II. Cell attachment to SB-fibrinogen and FMB (%)[a]

Cells	SB-Fibrinogen	FMB
Human fibroblasts	70	>95
Murine fibroblasts	82	>95
Human keratinocytes	0	0
Porcine smooth muscle cells	75	>95
Bovine endothelial cells[b]	>95	>95
Pig kidney epithelial cells	ND	>95
3T3/NIH fibroblasts	90	>95
OV-1063 human ovarian carcinoma cells	0	10
EMT-6 murine mammary carcinoma cells	62	94
4T1 murine mammary carcinoma cells	>90	>90
Human melanoma cells	>90	>90
J-774.2 Murine macrophage-like cells	0	0

[a]SB with covalently bound fibrinogen (SB-Fib) or FMB were placed on nearly confluent culture and the percentage of beads attached to the cells at day 3 was counted. Naked SB did not attach (O percentage).

[b]Different batches of endothelial cells show a wide range of responses.

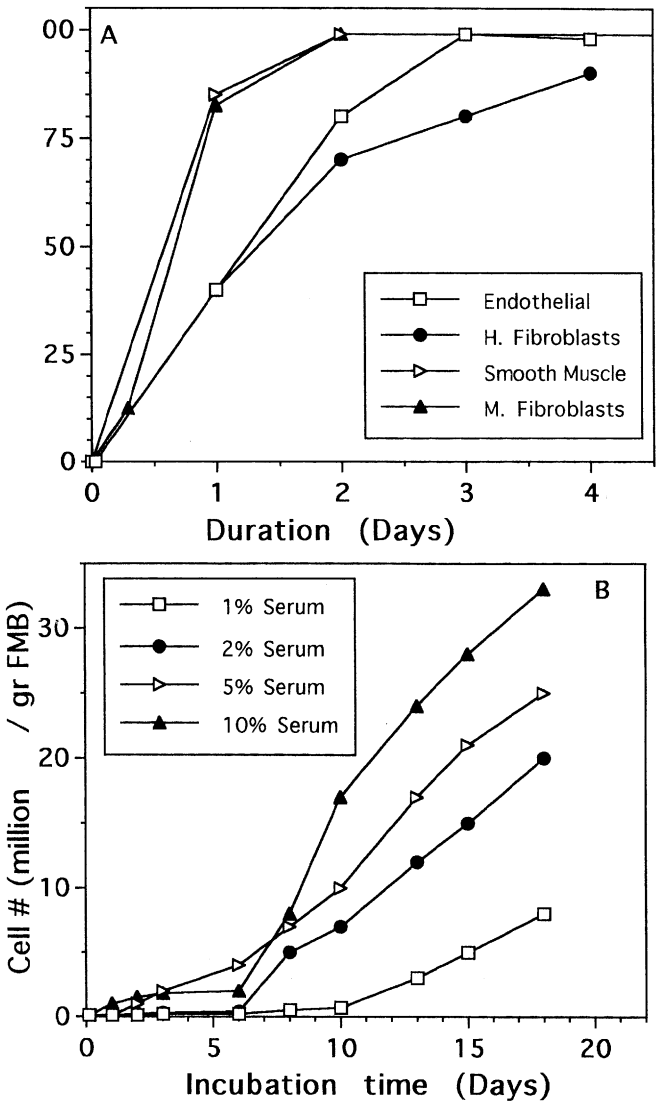

Figure 2. Responses of cells to FMB. (*A*) Rates of FMB attachment (haptotaxis) to fibroblasts, smooth muscle, and endothelial cells. The percentage of the FMB that were attached to the cultured cells at different time points was monitored by light microscopy. Standard errors of the measurements were in the range of 3%–8%. Endothelial cells and mouse fibroblasts attached to FMB much faster than fibroblasts and smooth muscle cells as seen following 24 and 48 h of incubation ($p < 0.05$). But similar degree of attachment was recorded at day 4 where binding of all the beads by the different cell types was reached. (*B*) Rates of proliferation of pig kidney epithelial cells. About 1 million cells were loaded on FMB and maintained at different media conditions. Cell number on FMB was evaluated by the MTS assay. By day 7 only the growth of cells in 1% serum was significantly different from the cell growth with other serum concentrations The difference in the growth of cells in different serum concentrations turned out to be fully significant ($p < 0.01$) from day 10 in the culture onwards.

The attachment and growth of cells on FMB was visualized by various microscopic techniques. By SEM, we could observe many fibroblasts attached on to a single bead with intimate contact between the cell membranes and the FMB in a manner where it was difficult to observe a boundary between the cell membrane and the surface of the microbead (**Fig 3**). **Figure 4**(*a*) shows a confocal microscopy image of a high titer (100 million cells per g FMB) of EMT-6 cells that were loaded on to FMB for 24 h. This image represents a composite of 50 optical slices through the FMB loaded with cells shown by their red-stained nuclei (about 8 μm in diameter). The number of cells attached to an average FMB (50–100 μm in diameter) ranged from 70 to 250 cells which

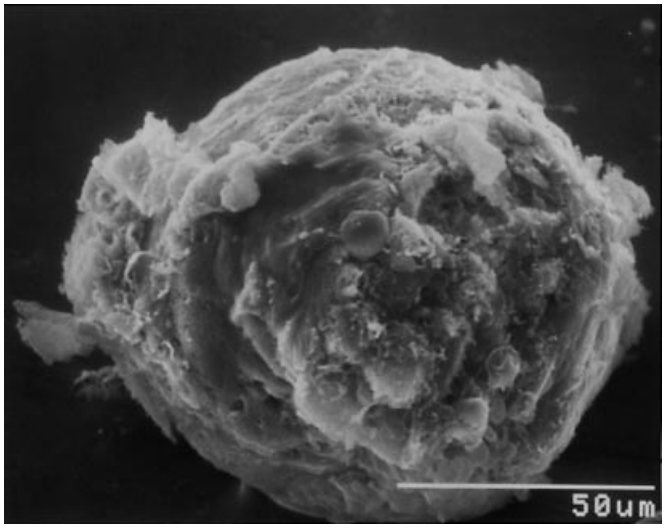

Figure 3. SEM of fibroblasts on FMB. The cell membranes appear to merge with the surface of the FMB.

typically were distributed over the whole surface and penetrated into invaginations in the FMB.

When HF were grown with smaller FMB (about 30 μm in diameter) for 3 d and observed by fluorescent microscopy, the cell visualized by their red-stained nuclei covered the FMB surfaces and appeared to aggregate the FMB into a tissue-like matrix with high cell density (**Fig 4*b***).

Cell transfer with FMB The downloading of HF from FMB that was embedded in a droplet of fibrin (20 mg per ml) on a tissue culture plate was studied. After 3 d of incubation, the red-stained nuclei of the cells could be seen by combined fluorescent and light microscopy to expand away from the densely populated FMB into the intermediate soft fibrin gel, leaving translucent vacuoles of digested gel (**Fig 4*c***, around lower bead—B2). Some of the migrating cells reached the area beyond the fibrin and settled on to the less populated plastic surface. This phenomenon was also visualized with confocal fluorescent microscopy, where the PI-stained nuclei revealed an expanding front of HF leaving the high cell density area on the FMB, while digesting the FMB and the surrounding fibrin gel (**Fig 4*d***).

^{31}P-NMR Fibroblast loaded FMB, placed in a perfused NMR tube, were monitored continuously for up to 24 h (**Fig 5**). A sensitive indicator of stress is the phosphocreatine (P_{Cr}) NMR signal (around 3 ppm). It gained in intensity immediately following the loading of the cells on FMB, reaching a maximum after about 3 h. The intensity remained constant thereafter and declined after 18 h. The corresponding intensity of the ATP β-phosphate resonances (–8.5 ppm) remained steady throughout the incubation period (24 h). Similar signal intensities were recorded for perfused mouse skin (data not shown).

Pig skin wound healing model Full thickness wounds were made on the paravertebral skin of outbred Yorkshire pigs and filled with human fibrin with or without other additives or cells, as described in the *Methods and Materials*. All wounds were harvested at day 3 a time when granulation tissue formation normally does not occur (Welch *et al*, 1990; Clark *et al*, 1996; McClain *et al*, 1996) before the onset of re-epithelialization. In wounds filled with only fibrin, modest fibroblast proliferation was noted in the subcutaneous tissue underlying the wounds (**Fig 6*A***). The number of fibroblasts, possibly accompanied with macrophages that could not be differentiated from the mass of fibroblasts in the granulation tissue, increased 2–3-fold when PDGF-BB was added to the fibrin (**Fig 6*B***). When cultured syngeneic fibroblasts suspended in exogenous fibrin were added to the wounds, fibroblast-like cells appeared singly disposed (**Fig 6*C***). In wounds receiving fibroblast

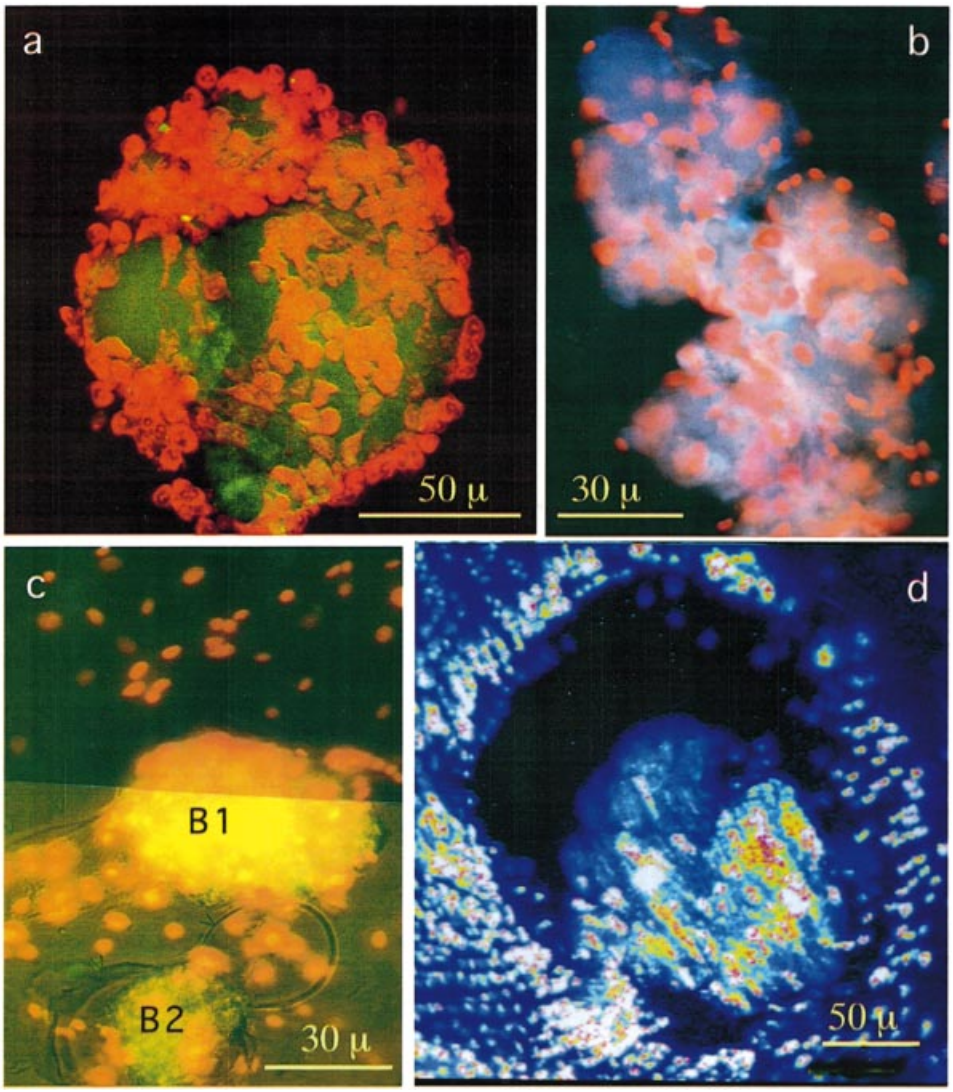

Figure 4. Micrographs of fibroblasts on FMB. (*a*) Confocal microscopy image of EMT-6 cells on a single FMB. The composite image of superimposed 50 optical slices reveals ≈200 cells loaded on a single FMB. (*b*) Fluorescent micrographs of HF, red PI-stained nuclei, grown on small FMB. The high cell density aggregated the beads to form a tissue-like structure. (*c*) A combined fluorescent and light microscopy image of cells loaded on FMB and embedded in low density fibrin droplet on a tissue plate. The upper part is a fluorescence image of the PI red-stained cell nuclei. The lower half of the image is combined fluorescent with light microscopy that shows the borders of the fibrin gel and the cells migrating from the FMB (*B1*) and (*B2*) with the transluscent outlines around *B2* that indicate the gel digestion track. (*d*) Composite superimposed slices taken by confocal microscopy of densely populated FMB as described in panel (*c*). The high intensity PI fluorescence of the nuclei show the position of cells digesting their way from the FMB and the surrounding fibrin.

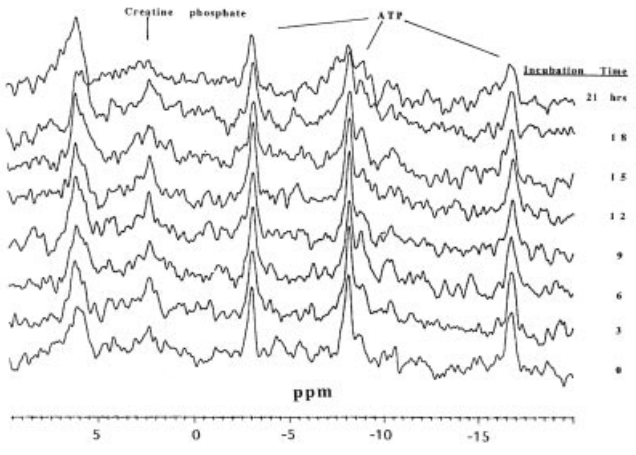

Figure 5. ^{31}P-NMR spectra of endothelial cells on FMB taken over a period of up to 24 h. The varied P_{Cr} signal (~ +3 ppm) indicate the stress induced consumption of the energy reserves of the cells. By contrast, the β-ATP signal at ~ –8 ppm reflect the cell viability within the period of the 21 h follow-up.

and PDGF-BB suspended in the fibrin, small pockets of granulation tissue were observed at the interface between the fibrin and the underlying subcutaneous tissue (**Fig 6*D***), as well as increased numbers of fibroblasts within the fibrin and the subcutaneous tissue. When only FMB were implanted in the wounds, they were easily visualized in the base of the wound in the newly formed granulation tissue (**Fig 6*E***). When PDGF-BB was included in the FMB suspension, a remarkable increase in the number of fibroblasts was noted at day 3 in the subcutaneous tissue underlying the wound (**Fig 6*F***). When FMB loaded with fibroblasts (10 million cells per g FMB) were applied into the wounds with fibrin, a loosely organized granulation tissue was observed at the interface between the FMB and the subcutaneous tissue (**Fig 6*G***). When PDGF-BB was also included, even greater amounts of more organized granulation tissue was observed (**Fig 6*H***). Thus, in all scenarios, FMB appeared to increase fibroblast proliferation compared with appropriate controls. When FMB were used as carriers for transplanted fibroblasts substantial granulation tissue occurred in 3 d wounds. Compared with FMB control (**Fig 6*E***), the size of the FMB 3 d after implant was significantly smaller where significant granulation tissue was formed (**Fig 6*F–H***). The biodegradation of the implanted FMB seemed to correlate with cell density of the granulation tissue. It should be noted that neovasculature indicative of angiogenesis was clearly noted in about 30% of the specimens in which fibroblasts on FMB had been added to the wounds without PDGF and in about 60% of the specimens in which fibroblasts on FMB had been added to the wounds with PDGF. Thus the tissue organization observed in specimens receiving these additives is granulation tissue, not simply fibroplasia.

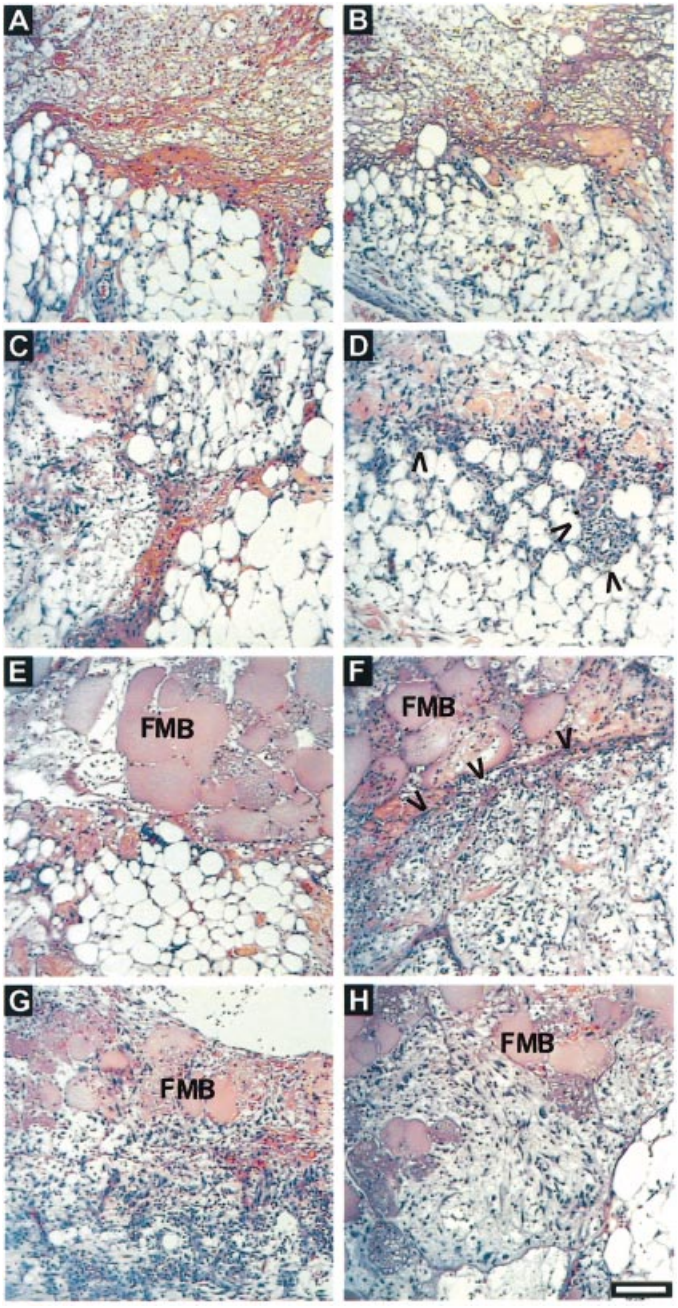

Figure 6. Pig skin wound healing (day 3). Histology of cutaneous wounds implanted with 3 mg per ml fibrin and combinations of FMB, human skin fibroblasts, PDGF-BB, and controls. (*A*) Wound with no addition other than human fibrin shows no evidence of granulation tissue. (*B*) Wound containing exogenous PDGF-BB shows increased fibroblast number beneath the wound, but no granulation tissue. (*C*) Wound to which fibroblasts suspended in fibrin were added, shows individual fibroblasts in the fibrin clot, but no granulation tissue. (*D*) Wound to which fibroblasts suspended in a fibrin + PDGF-BB were added, shows nascent granulation tissue at the bottom of the wound (*arrows*) as well as increased numbers of individual fibroblasts in the fibrin clot. (*E*) Wound to which FMB suspended in fibrin were added, shows FMB along the base of the wound. (*F*) Wound to which FMB suspended in fibrin + PDGF-BB solution were added, shows FMB along the base of the wound and a great number of fibroblasts in the underlying subcutaneous tissue (*arrows*). (*G*) Wound to which fibroblast loaded FMB suspended in fibrin were added, shows FMB along the base of the wound. A large number of fibroblasts were observed between the FMB and the underlying subcutaneous tissue. (*H*) Wound to which fibroblasts loaded FMB suspended in fibrin and PDGF-BB were added, shows FMB along the base of the wound and robust granulation tissue between the FMB and in the underlying subcutaneous tissue. *Scale bar:* 100 μm.

DISCUSSION

Substrates that can be used to grow cells are essential for a wide range of applications ranging from advanced tissue culture techniques to tissue engineering for transplantation. Based on our experience with fibrin sealant and the haptotactic attraction of cells to fibrin (Gorodetsky *et al*, 1998), we developed biodegradable FMB that were essentially composed of partially heat denatured fibrin(ogen), cross-linked by the endogenous transglutaminating activity of factor XIII. For example, fibrinogen denatures above 50°C due to the instability of the D-domains, whereas factor XIIIa is much more stable and can cross-link proteins at higher temperatures. Advantage of this was taken by activating fibrinogen and factor XIII with a low level of thrombin, then injecting the mixture into moderately heated oil. After processing, we obtained insoluble, mechanically stable FMB 50–200 μm in diameter, without utilizing chemical cross-linking reagents (such as glutaraldehyde) which would inactivate biologically active epitopes of the proteins. Whereas we originally prepared FMB from purified components, we could also prepare FMB from cryoprecipitate which contains other proteins to which cell are attracted such as fibronectin and von Willebrand factor (**Table I**). We thereby obtained insoluble protein microbeads which retained the biologic effects of fibrin(ogen).

Haptotactic tests indicated that normal and transformed cells which responded to Sb-Fib, also attached to FMB. These include fibroblasts, endothelial, smooth muscle, EMT-6 cells and cultured primary human melanoma cells (**Table II**, **Fig 2**). By comparison, keratinocytes and leukemic cells (J-774.2 and p-388) did not bind or attach to any of the substrates. It would seem that cells require appropriate cell receptors to fibrinogen in order to attach onto the FMB.

The growth of normal cells (kidney epithelial) loaded on FMB appeared to be optimal with 10% serum in the culture medium (**Fig 2*B***), although the cells grown on the FMB in lower serum concentrations still were able to proliferate significantly, but at a slower rate. Similar growth patterns on FMB were recorded with other cell types.

Very high cell density on FMB could be achieved. When appropriately perfused with medium with nutrients and gas mixture, the cells appeared fully viable and functional. This was reflected by phosphate signals (i.e., ATP, P_{Cr}) as monitored by ^{31}P-NMR. For example, the phosphate signals generated at the high endothelial or fibroblast cell density (100 million cells per g FMB) was equivalent to the signal obtained from normal tissues (data not shown). Even with full perfusion with medium and aeration, cells on FMB required some 3 h to recover from the stress of being transferred into the NMR set-up. Thereafter, the P_{Cr} signal was stronger, only decaying after 18 h (**Fig 5**). These changes were possibly due to factors associated with cell stress in the first phase of their loading into the NMR system and difficulties of maintaining cells in this system for a prolonged time. Notwithstanding, the steady ATP ^{31}P signals indicated that the cells were fully viable.

Confocal microscopy provided detailed images of cells attached to and growing on FMB. The cells on FMB appeared to exhibit minimal contact inhibition and were capable of achieving extremely high density (100 million cells per g FMB) for extended periods. The cells loaded on FMB could subsequently be transferred to tissue culture plates, either directly or embedded in fibrin gel (**Fig 4**). The self-downloading of cells from highly populated FMB to the transfer site, directly or through the digestion of embedding fibrin gel, suggests a wide range of application for FMB in cell transplantation.

Wounds in human skin as well as in the pig model heal through the formation of granulation tissue which is rarely manifested prior to the fourth day after wounding. In the pig skin dermal wound model, by day 3, only wounds which had been implanted with the combination of FMB + fibroblasts demonstrated accelerated healing and substantial formation of granulation tissue. PDGF-BB, a potent growth factor (Koyama *et al* 1994), did not substantially

accelerate wound healing at this early time point except when combined with FMB loaded with fibroblasts (**Fig 6**). The advantage of fibroblasts transplanted on FMB may, in part, be attributed to their dense composition, which facilitates settling to the wound base and thereby allows proper cell orientation within the wound bed. The observation that FMB appeared to be much smaller 3 d after their transplantation with cells (**Fig 6*E–H***) corresponds to our tissue culture experiments wherein the FMB were rapidly biodegraded (**Fig 4*c, d***). Our positive results with the skin wound system indicate that implanted FMB with or without cells have great advantages over current approaches for enhancing wound healing in skin and possibly for regenerating other tissues.

In conclusion, we describe the characteristics of biodegradable FMB with a number of projected uses. FMB stimulate cell migration and permit cell proliferation. They could be used as a matrix to grow cells, as well as a vehicle to transfer cultured cells from one milieu to another. The high density of cells on FMB seems to be associated with the exposure of haptotactic epitopes of the partially denatured fibrinogen. The porosity of the beads provides a high surface area for cell attachment and growth. The insolubility of the FMB and their biodegradable nature make them an ideal provisional matrix for tissue engineering and cell transplantation. We are currently studying mechanistic details of cell attraction to fibrinogen-derived matrices which will expand the uses of FMB for wound healing and tissue engineering.

This work is dedicated to Elisha Berman who passed away just prior to publication. He was a friend as well as a professional collaborator. His generosity in materials and personal encouragement in this and other projects was genuine. He will be missed by all. This study was supported in part by a grant from the Basic Research Fund of the Israel Academy of Sciences (RG). We wish to thank Dr. Marc Tarshish (Hadassah Medical School Interdepartmental facility) for his advice and help with the confocal microscopy, and Dr. Ron Goedin and Norman Katz (Department of Pathology, Mt. Sinai Medical Center, New York, NY) for technical assistance with electron microscopy of samples.

REFERENCES

Arshady R: Microspheres and microcapsules, a survey of manufacturing techniques. *Polymer Eng Sci* 30:905–914, 1990

Bar-Shavit R, Benezra M, Eldor A, Hy-Am E, Fenton JW, Wilner GD, Vlodavsky I: Thrombin immobilized to extracellular matrix is a potent mitogen for vascular smooth muscle cells: nonenzymatic mode of action. *Cell Regul* 1: 453–463, 1990

Brown LF, Lanir N, McDonagh J, Tignazzi K, Dvorak AM, Dvorak HF: Fibroblast migration in fibrin gel matrices. *Am J Pathol* 142:273–283, 1993

Clark RAF, Tonnesen MG, Gailit J, Cheresh DA: Transient functional expression of avb3 on vascular cells during wound repair. *Am J Pathol* 148:1407–1421, 1996

Daniel TC, Gibbs VC, Milfay DF, Garovoy MR, Williams LT: Thrombin stimulates c-cis gene expression in microvascular endothelial cells. *J Biol Chem* 261: 9579–9582, 1986

Dawes KE, Gray AJ, Laurent GJ: Thrombin stimulates fibroblast chemotaxis and replication. *Eur J Cell Biol* 61:126–130, 1993

Evans R: Biodegradable parental (albumin) microspherules. US Patent 3 663 687, 1972

Gorodetsky R, Vexler A, An J, Mou X, Marx G: Chemotactic and growth stimulatory effects of fibrin(ogen) and thrombin on cultured fibroblasts. *J Lab Clin Med* 131:269–280, 1998

Gray AJ, Bishop JE, Reeves JT, Laurent GJ: Aα and Bβ chains of fibrinogen stimulate proliferation of human fibroblasts. *J Cell Sci* 104:409–403, 1993

Gref R, Minamitake Y, Peracchia MT, Trubetskoy V, Torchilin V, Langer R: Biodegradable long circulating polymeric nanospheres. *Science* 263:1600–1603, 1994

Griffith B, Looby D. Scale-up of suspension and anchorage-dependent animal cells. In: Pollard JW, Walker JM (eds). *Methods in Molecular Biology*, Vol. 75. *Basic Cell Culture Protocols*. Totowa, NJ: Humana Press, 1997

Koyama N, Hart CE, Clowes AW: Different functions of the platelet-derived growth factor: a- and b-receptors for the migration and proliferation of cultured baboon smooth muscle cells. *Circ Res* 75:682–691, 1994

Lee TK, Sokolovski TD, Royer GP: Serum albumin beads: an injectable, biodegradable system for the sustained release of drugs. *Science* 213: 233–235, 1981

Lorenzet R, Sobel JH, Bini A, Witte LD: Low molecular weight fibrinogen degradation products stimulate the release of growth factors from endothelial cells. *Thrombosis Haemostasis* 68:357–363, 1992

Marx G, Mou X, Freed R, Ben-Hur E, Yang C, Horowitz B: Protecting fibrinogen with rutin during UVC irradiation for viral inactivation. *Photochem Photobiol* 63:541–546, 1996

McClain SA, Simon M, Jones E, *et al*: Mesenchymal cell activation is the rate limiting step of granulation tissue formation. *Am J Pathol* 149:1257–1270, 1996

Miyazaki S, Hashiguchi N, Takeda M, Hou WM: Antitumor effect of fibrinogen microspheres containing doxorubicin on Ehrlich ascites carcinoma. *J Pharm Pharmacol* 38:618–620, 1986a

Miyazaki S, Hashiguchi N, Hou WM, Yokouchi C, Takeda M: Preparation and evaluation in vitro and in vivo of fibrinogen microspheres containing adriamycin. *Chem Pharm Bull* 34:3384–3393, 1986b

Miyazaki S, Hashiguchi N, Sugiyama M, Takeda M, Morimoto Y: Fibrinogen microspheres as novel drug delivery systems for antitumor drugs. *Chem Pharm Bull* 34:1370–1378, 1986c

Royer GP: Implants, microbeads, microcapsules, preparation thereof and method for administering a biologically-active substance to an animal. US Patent 4 349 530, 1982

Sanders RP, Goodman NC, Amiss LR, *et al*: Effect of fibrinogen and thrombin concentrations on mastectomy seroma prevention. *J Surg Res* 61:65–70, 1996

Sharoni R, Olivson A, Chandra M, *et al*: A ^{31}P NMR study of preconditioned isolated perfused rat heart exposed to intermittent ischemia. *Magn Res Med* 36:66–71, 1996

Shuman F: Thrombin–cellular interactions. *N Y Acad Sci* 408:228–235, 1986

Welch MP, Odland GF, Clark RAF: Temporal relationships of F-actin bundle formation, collagen and fibronectin matrix assembly, and fibronectin receptor expression to wound contraction. *J Cell Biol* 110:133–145, 1990

Yapel AF: Albumin microspheres: Heat and chemical stabilization. *Methods Enzymol* 112:3–43, 1985

Zou J, Hamman J, Marx G, Horowitz B: Method for activating prothrombin to thrombin. *US Patent* 5, 677, 162, 1997